Earthquake Induced Damage Mitigation from Soil Liquefaction

CLASS A PREDICTION FOR LIQUEFACTION REMEDIATION INITIATIVE CENTRIFUGE TEST 8 (LRICT8)

By:
Ahmad Jafari

Supervisor: Dr. Radu Popescu

Memorial University of Newfoundland

MARCH 2005

Introduction

In this report Class A prediction of the 8th LRI (Liquefaction Remediation Initiative) centrifuge test (LRICT8) is presented and discussed.

LRICT8 geometry and input motion

General layout and input motion used for class A prediction of LRICT8 are similar to those of LRICT5 as shown in Figures 1 and 2. The slope has an inclined silt layer with a slope of 1:5.7 and the mitigation strategy includes three drainage dykes as indicated in Figure 1. The input acceleration time history used in this test is A2475 with a magnification factor of 2, i.e. 2×A2475 as shown in Figure 2. The FE model for this prediction is shown in Figure 3. The model consists of 588 nodes and 542 elements.

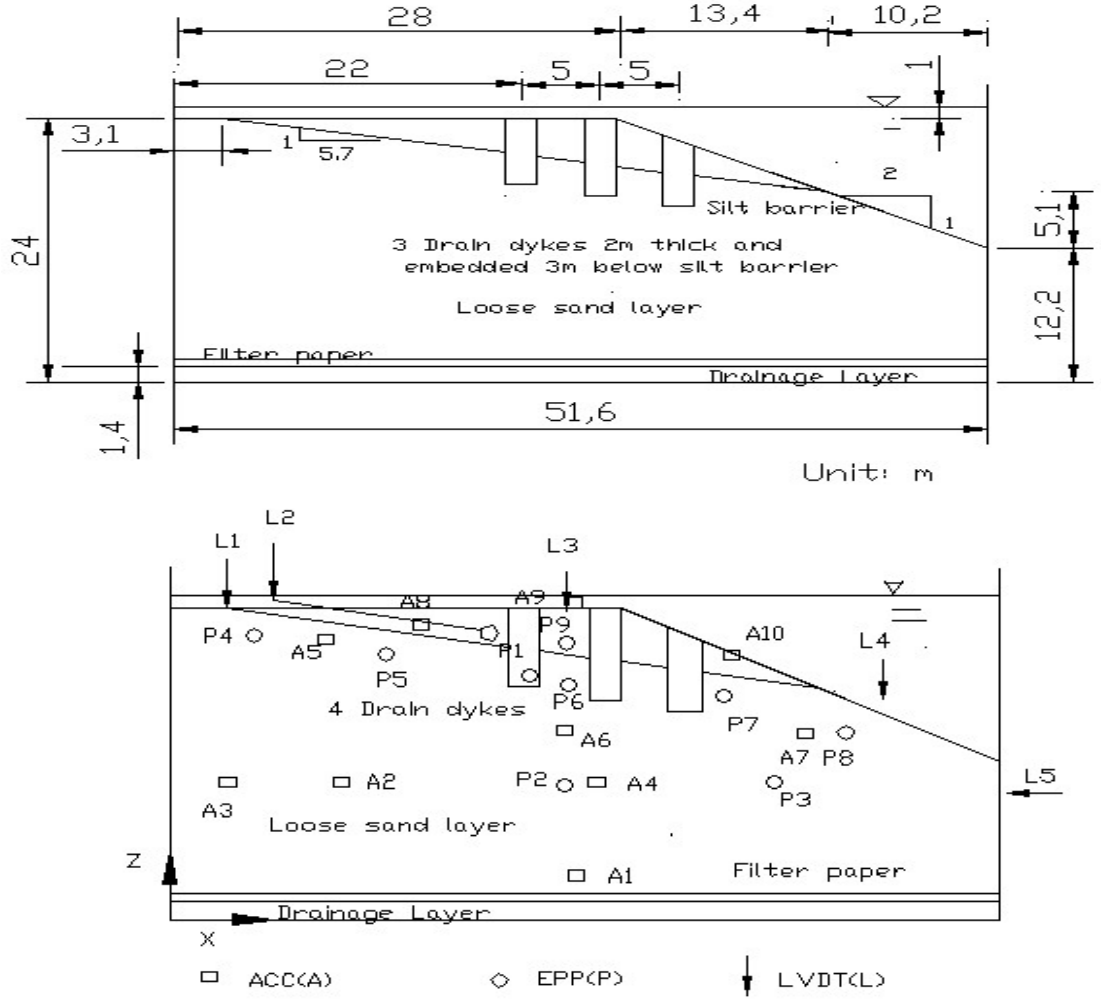

Fig.1 Geometry and instrumentation layout of LRICT8 given by C-CORE

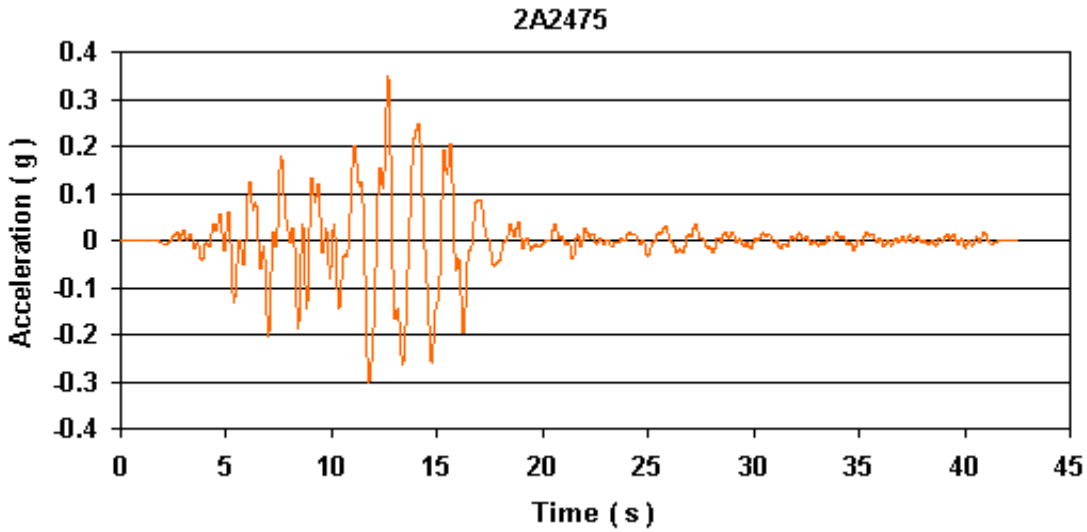

Fig. 2 Input acceleration time history used for class A prediction of LRICT8

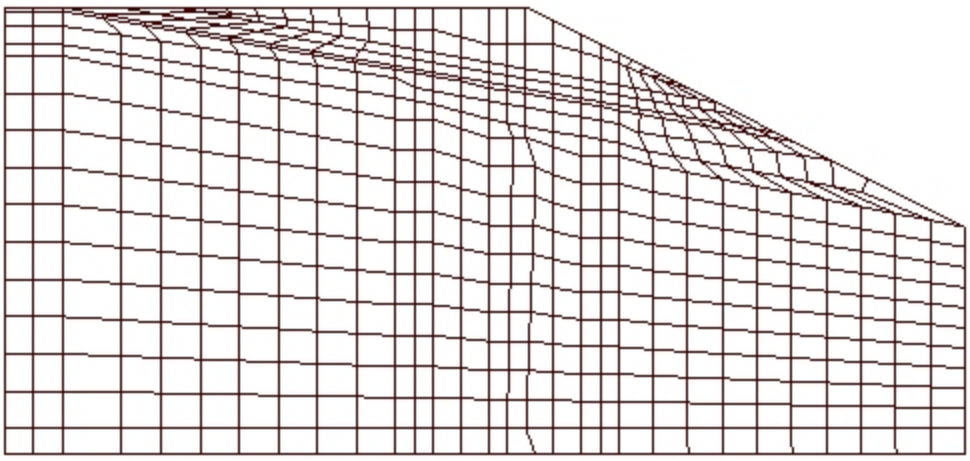

Fig. 3 FE mesh used in class A prediction of LRICT8

Soil properties

All the required sets of soil constitutive parameters for different materials used in class A prediction of LRICT8 have already been reported in the previous class A predictions. Table 1 includes a summary of these sets of parameters and their corresponding reference reports.

Constitutive parameters	Materil properties and their corresponding reference report			
	Loose sand (LRICT4 class A)	**Drainage dyke** (LRICT4 class A)	**Silt** (LRICT7 class A)	**Looser sand** (LRICT7 class A)
ρ_s (kg /m^3) n^w k (cm / s)	2710 0.448 0.0084	2670 0.423 0.84	2670 0.448 0.0000084	2710 0.467 0.0084
G_0 (MPa) p_0 (KPa) n ν	45 100 0.5 0.3	45 100 0.5 0.3	5 100 0.8 0.4	15 100 0.5 0.3
ϕ k_0 ε^{max}_{dev}	39^o 1 0.02(C), 0.01 (E)	41^o 1 0.02(C), 0.01 (E)	25^o 1 0.06 (C), 0.06 (E)	35^o 1 0.02 (C), 0.01 (E)
ψ X_{PP}	34^o 0.27	34^o 0.27	17^o 0.01	34^o 0.55

Table 1. Soil constitutive parmeters used in class A prediction of LRICT8

Results of Class A prediction of LRICT8

Results of class A prediction of LIRCT8 are shown in Figures 4 to 26 at prototype scale as predicted displacements, excess pore pressure ratios, and accelerations for all transducer positions. For 10 s < t < 20 s, the numerical model predicts significant plastic dilation at shallow locations (manifested as large negative excess pore water pressures at EPP4, EPP8, and EPP9). The predicted contours of maximum shear strain at the end of analysis (t=42.54 s) for both LRICT7 and LRICT8 are shown in Figure 27 along with the deformed shapes of the models. It is predicted that the presence of the drains in LRICT8 significantly reduces the possibility of general slope failure (large lateral displacement), as predicted and observed in CT7. As it can be seen in Figure 27, in the case of LRICT7, nearly the entire interface between the silt layer and looser sand experiences very large strains (up to 80%). On the other hand, in LRICT8 strains are remarkably lower; however, still large shear strains (larger than 30%) are predicted to occur only at the area around the intersection of the silt layer and the model external slope. This difference indicates the effectiveness of the mitigation strategy used in LRICT8. Figures 28 to 32 show contours of excess pore water pressure ratios at different instants. The large

oscillating pressures shown by the contours near the left boundary are the result of boundary effects (presence of the rigid lateral wall of the box). As it can be seen from these figures, excess pore water pressures are predicted to be insignificant at locations close to the drainage dykes (e.g., see EPP1, EPP6 and EPP7 time histories). However, in the free field upslope, significant increase in excess pore water pressure below the silt layer is predicted after the end of earthquake, i.e. after about t = 20 s (e.g., see EPP5 time history). Figure 33 shows the predicted vertical displacement contours at the end of analysis (t = 42.54 s). It is predicted that in the free field upslope settlements are higher than 0.6 m.

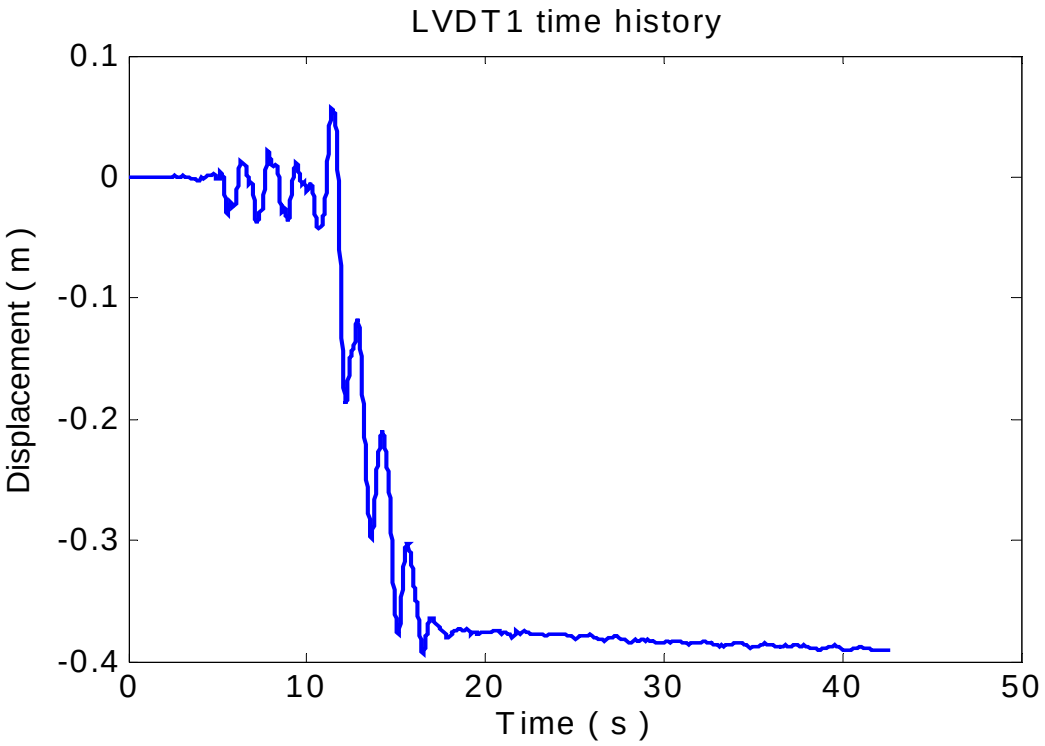

Fig. 4 Predicted LVDT1 time history

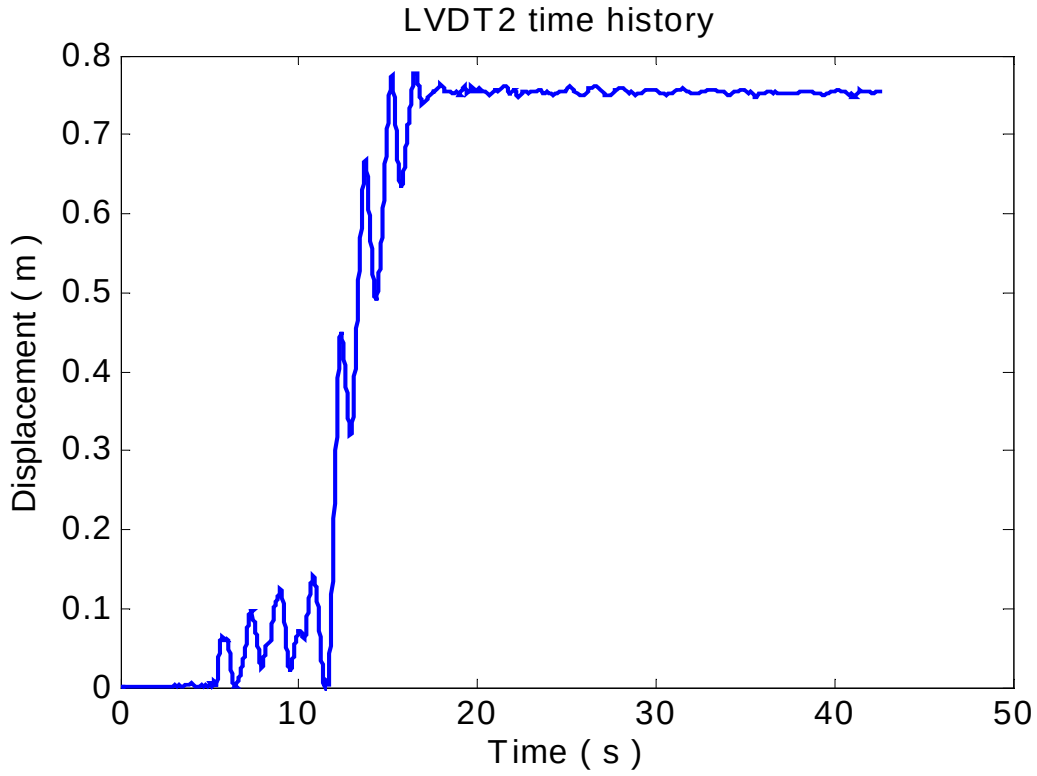

Fig. 5 Predicted LVDT2 time history

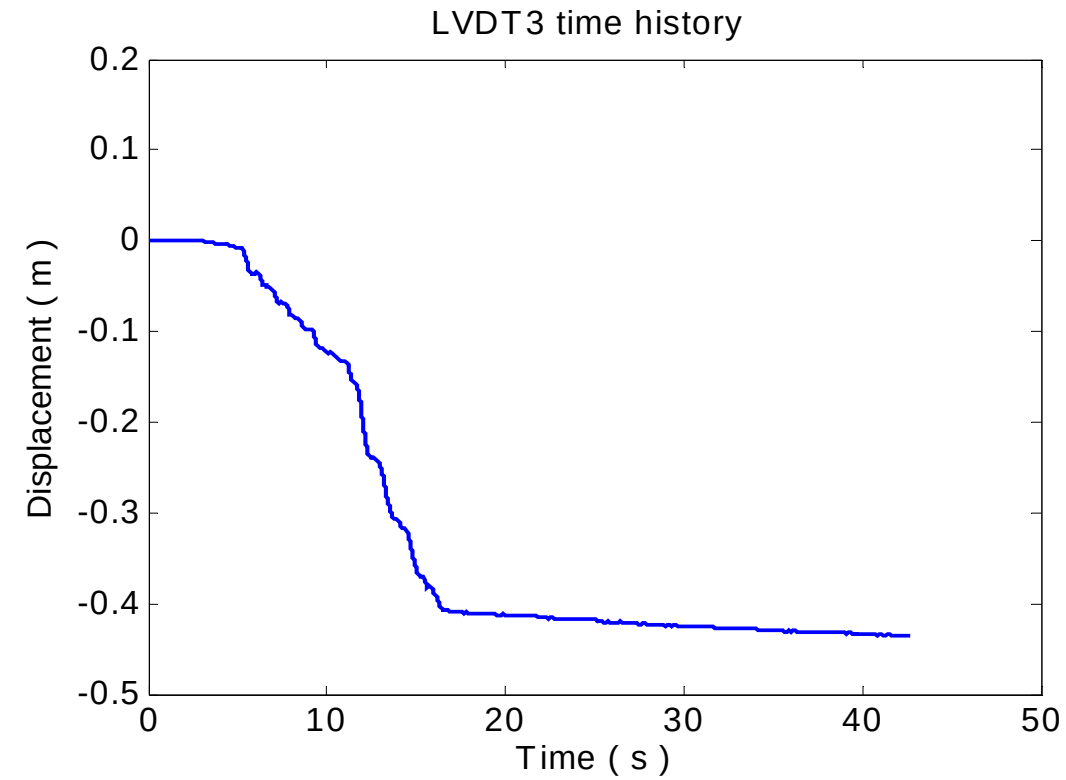

Fig. 6 Predicted LVDT3 time history

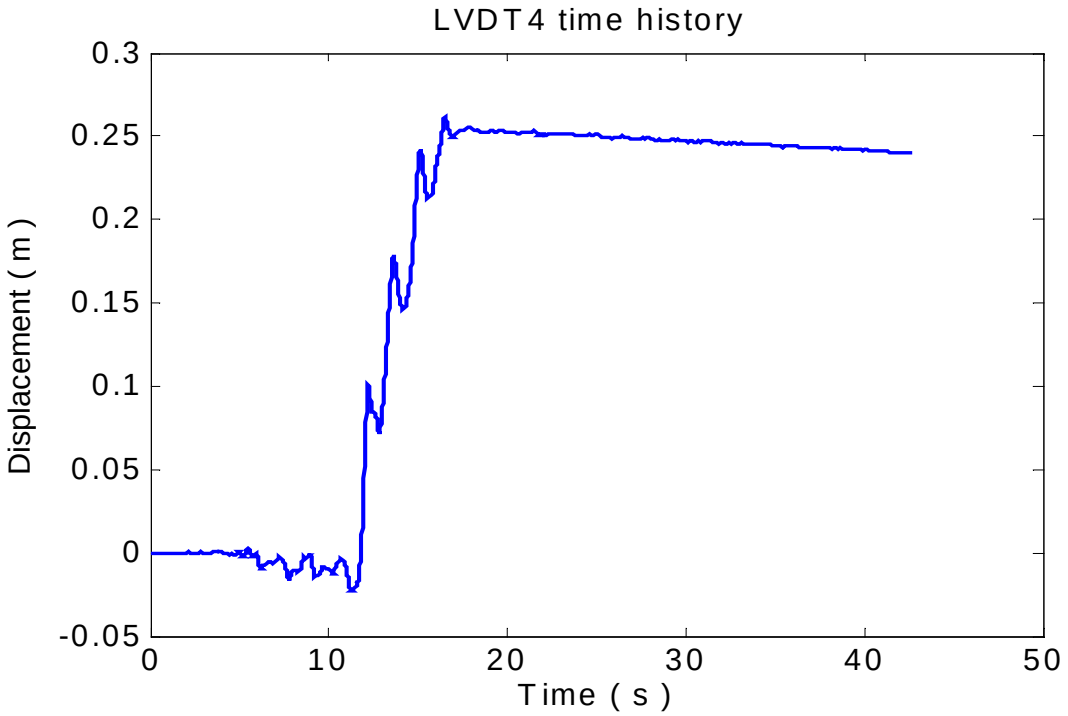

Fig. 7 Predicted LVDT4 time history

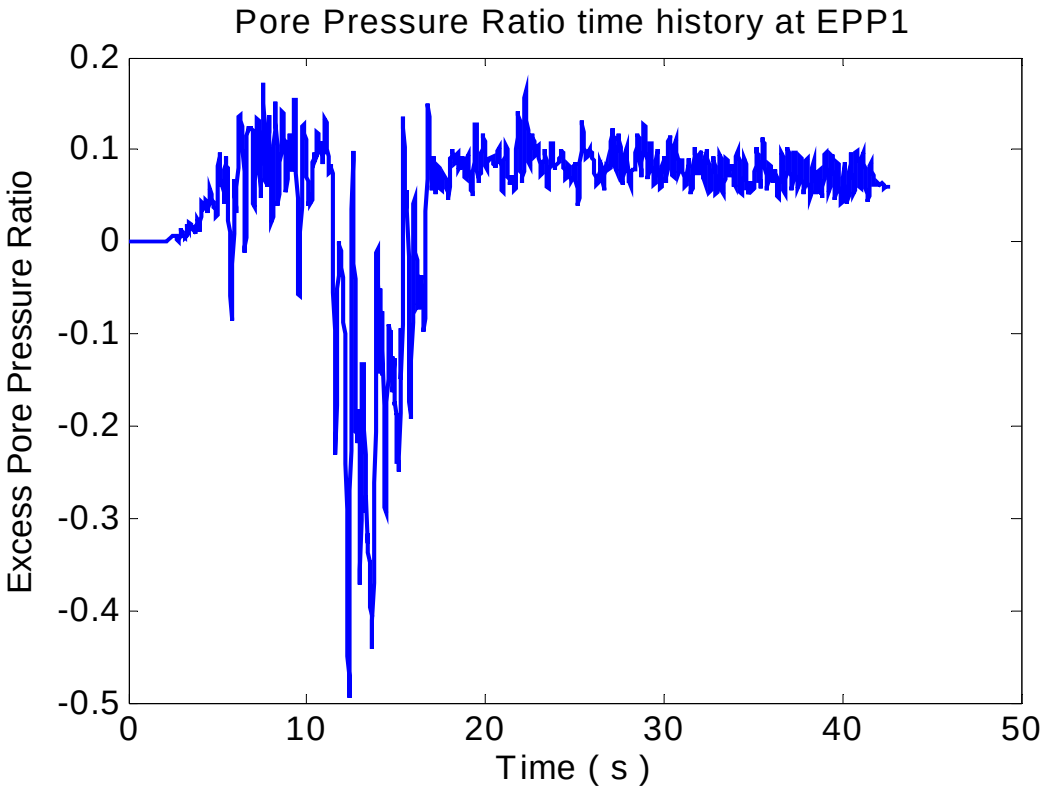

Fig. 8 Predicted EPP1 time history (IVES=51 KPa)

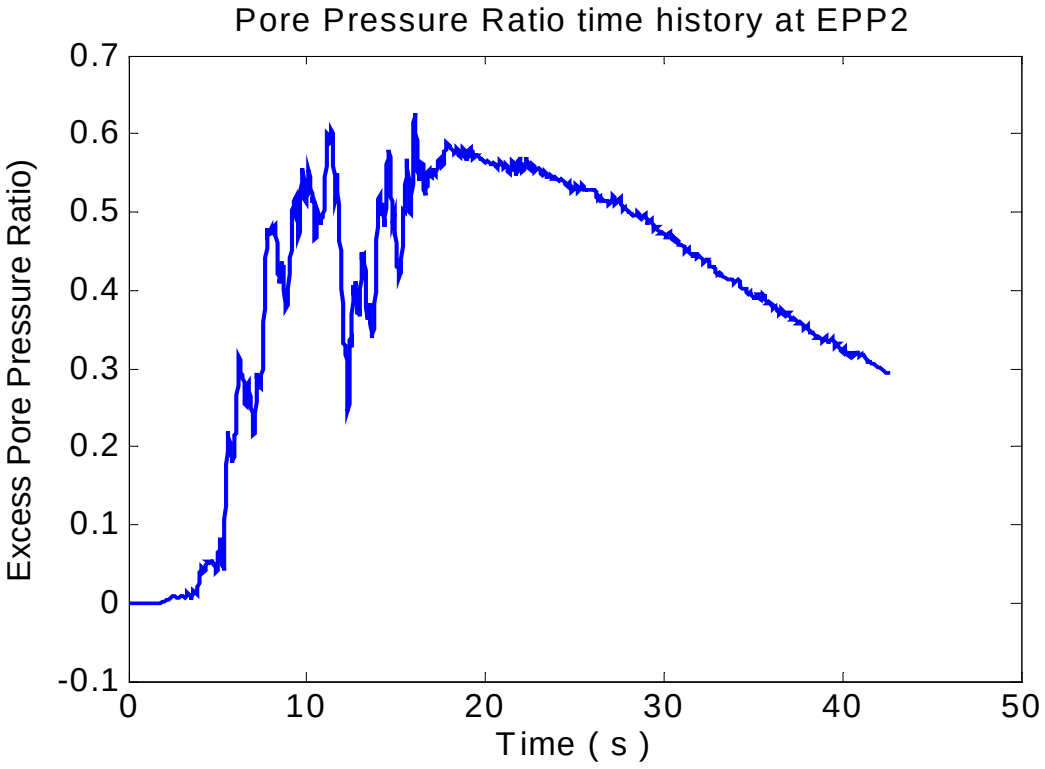

Fig. 9 Predicted EPP2 time history (IVES=121 KPa)

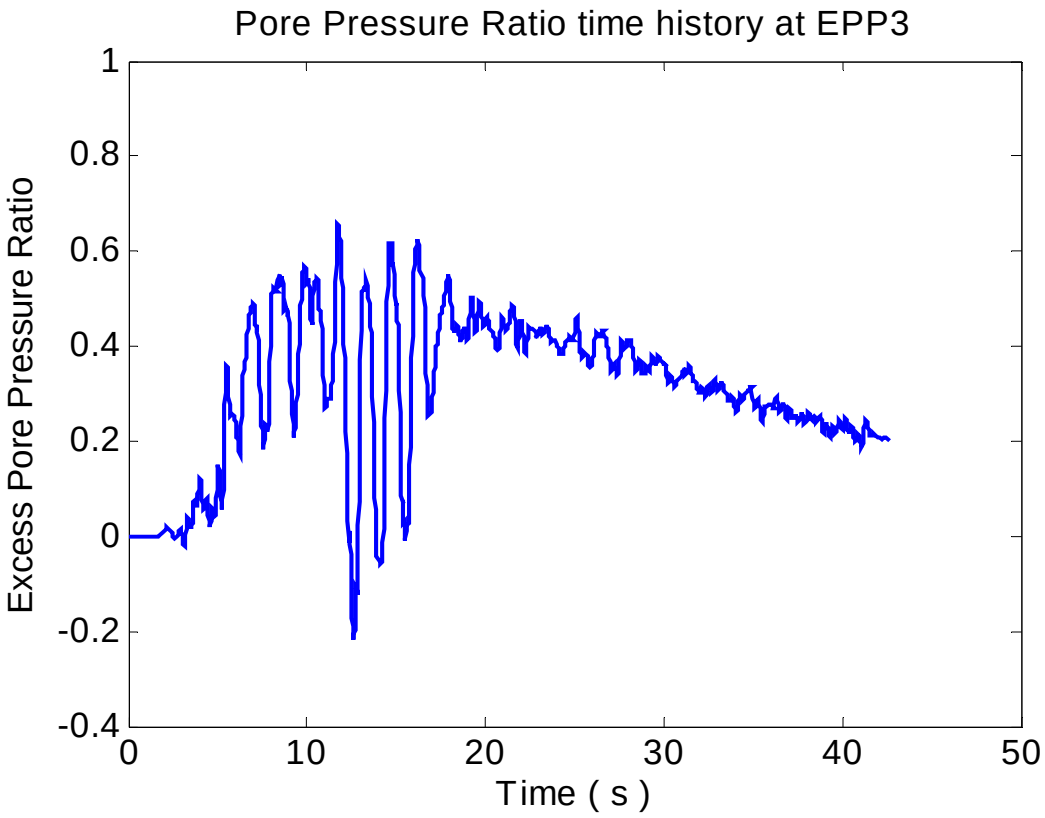

Fig. 10 Predicted EPP3 time history (IVES=88 KPa)

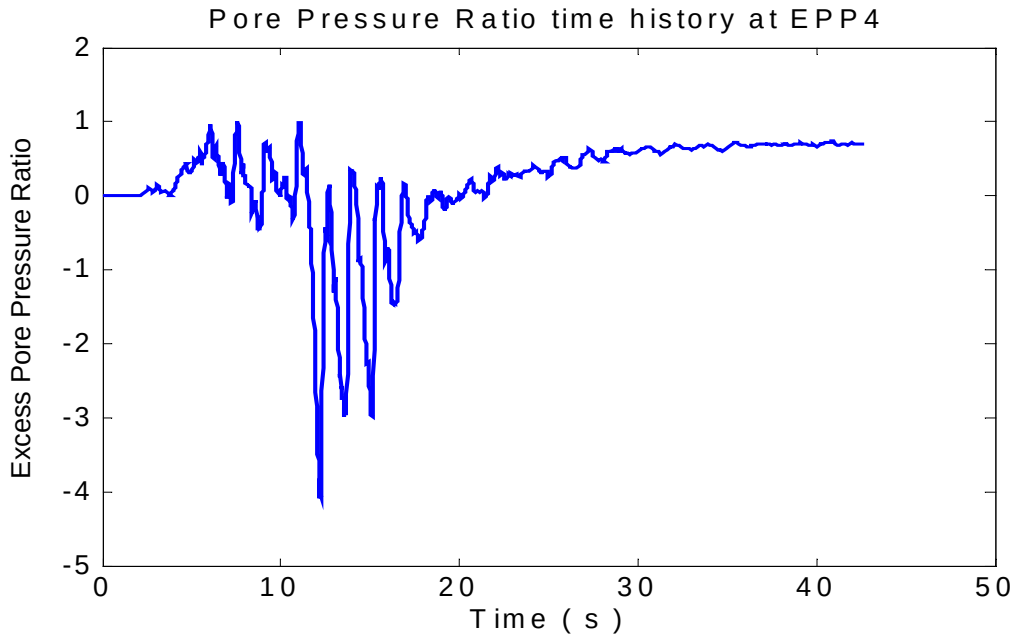

Fig. 11 Predicted EPP4 time history (IVES=12 KPa)

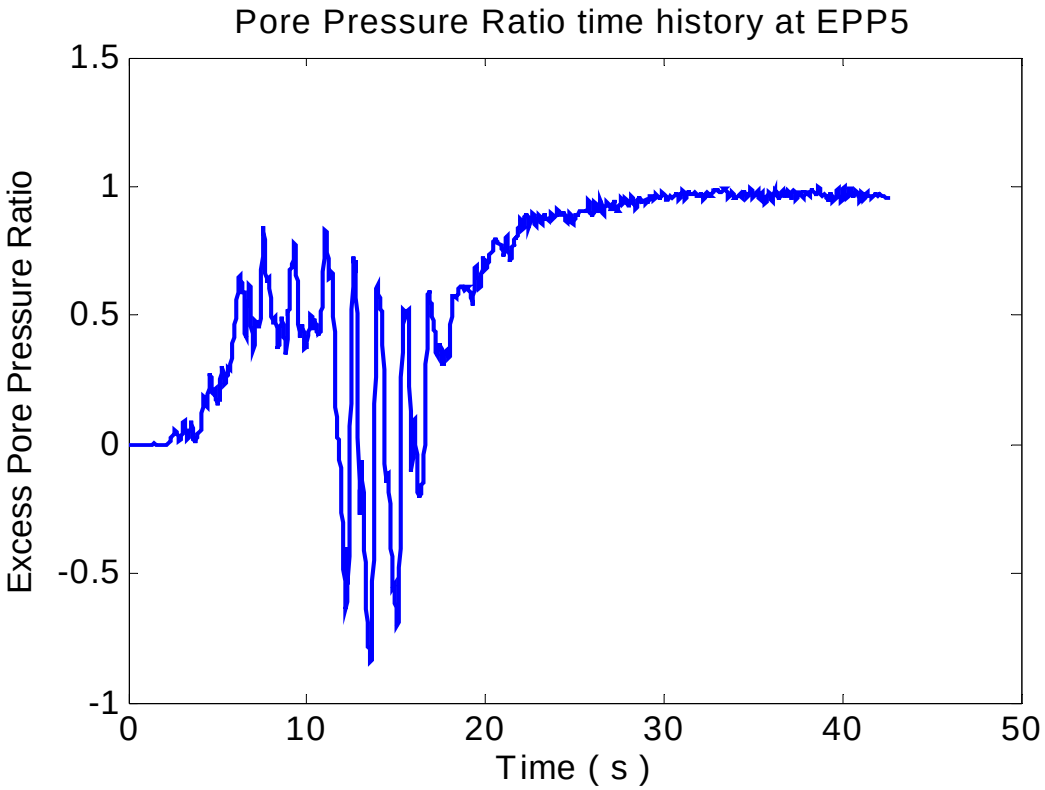

Fig. 12 Predicted EPP5 time history (IVES=31 KPa)

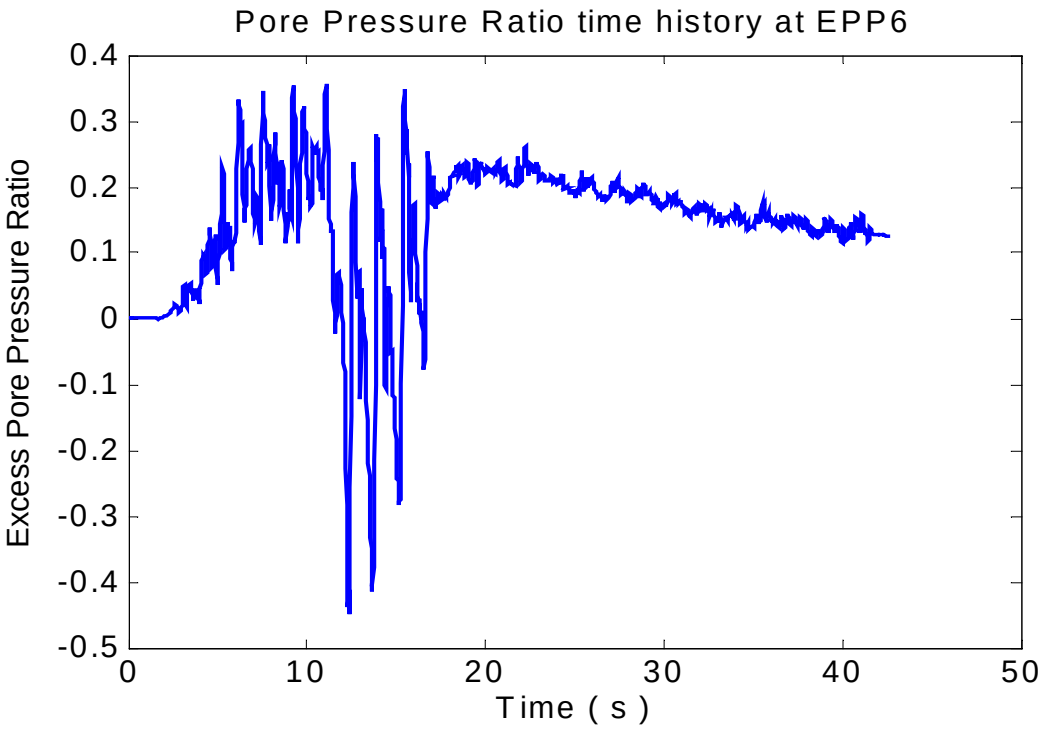

Fig. 13 Predicted EPP6 time history (IVES=47 KPa)

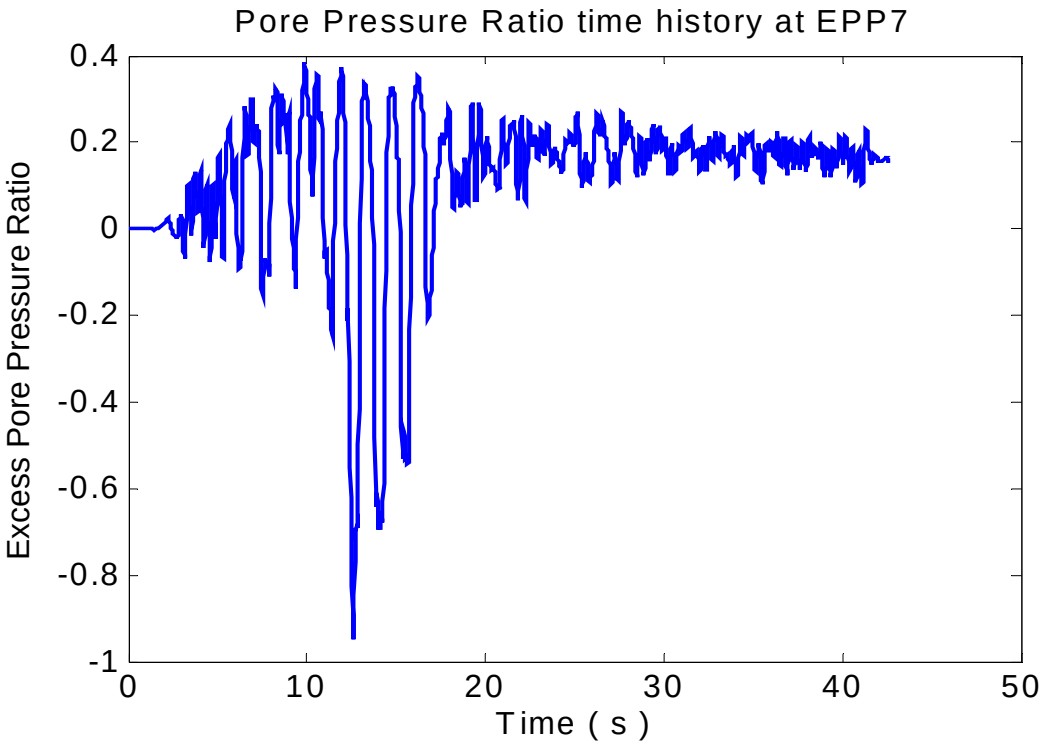

Fig. 14 Predicted EPP7 time history (IVES=44 KPa)

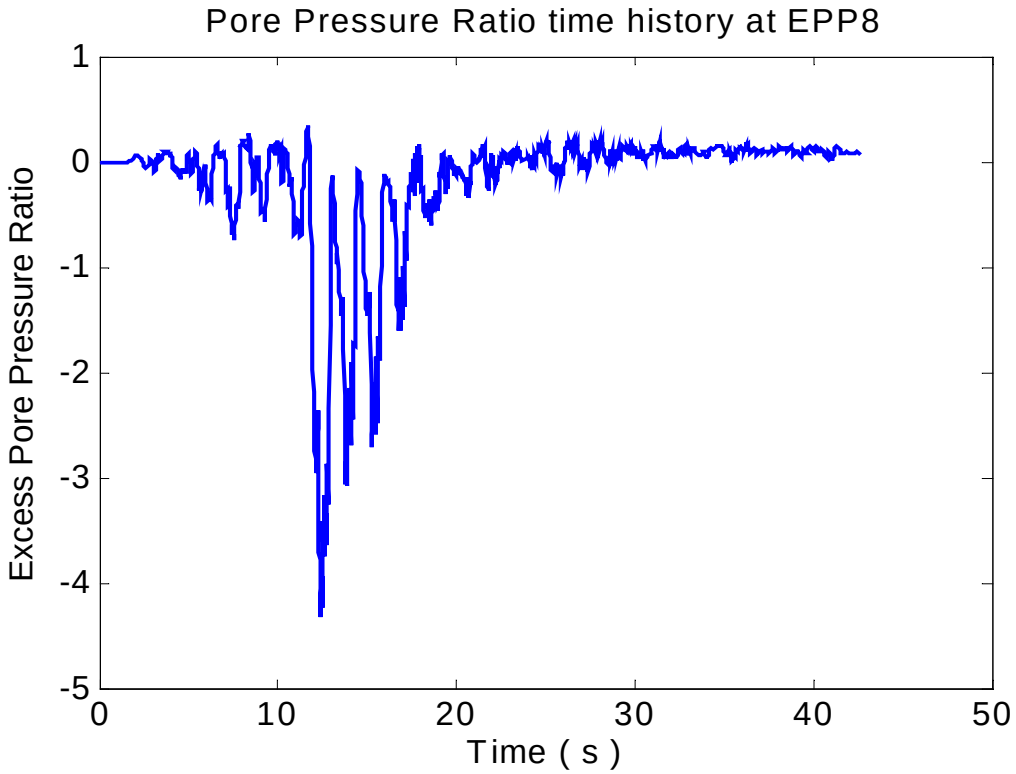

Fig15 Predicted EPP8 time history (IVES=14 KPa)

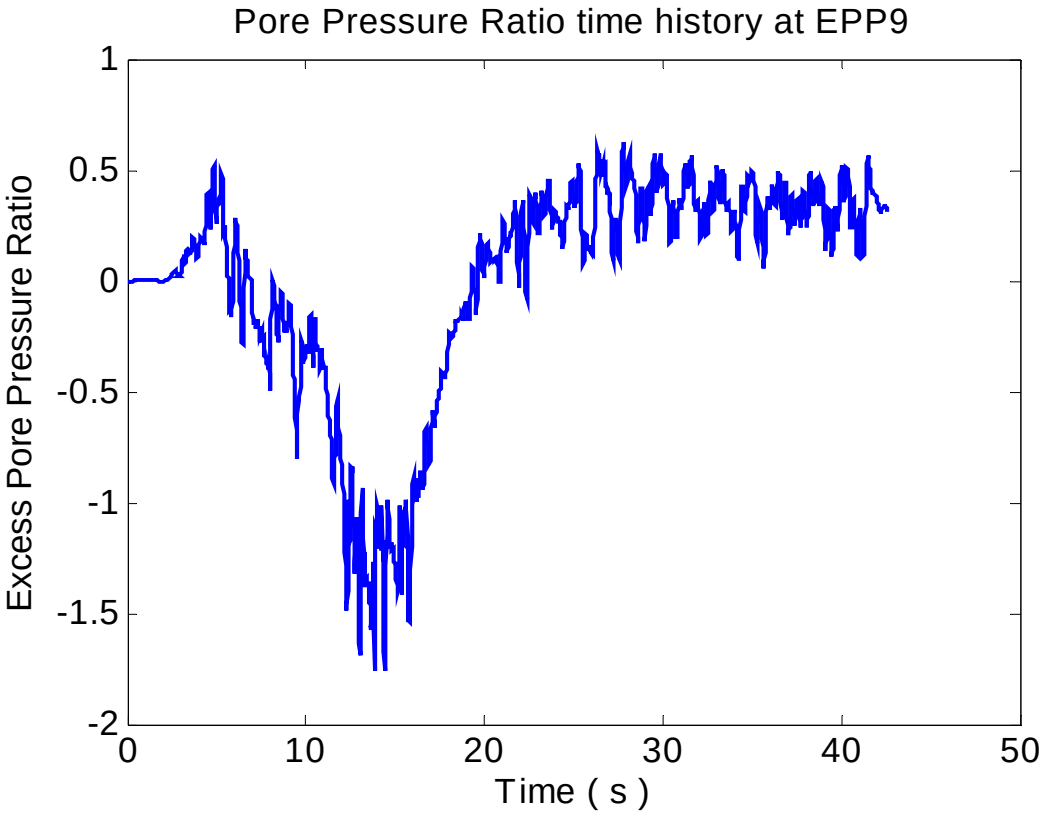

Fig. 16 Predicted EPP9 time history (IVES=14 KPa)

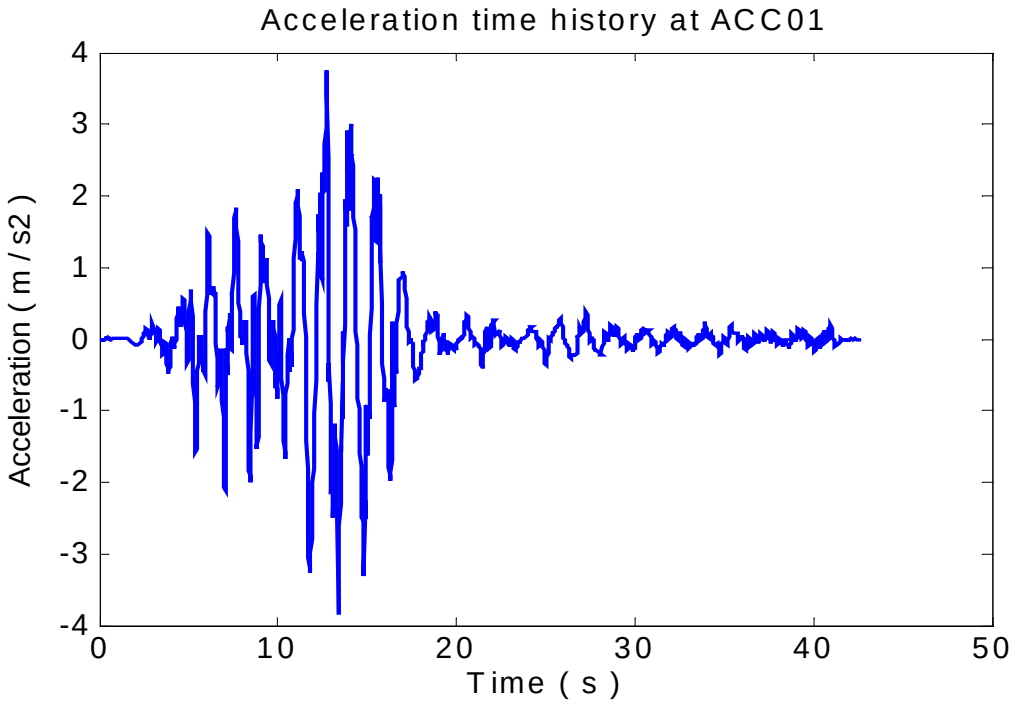

Fig. 17 Predicted ACC01 time history

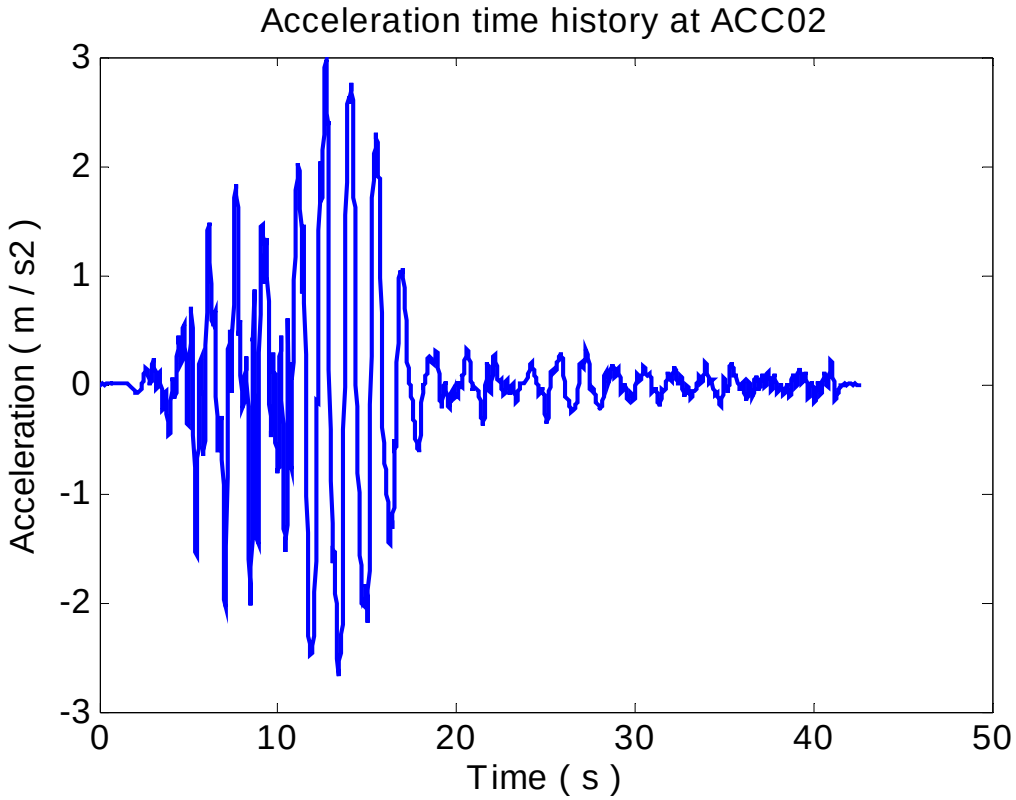

Fig. 18 Predicted ACC02 time history

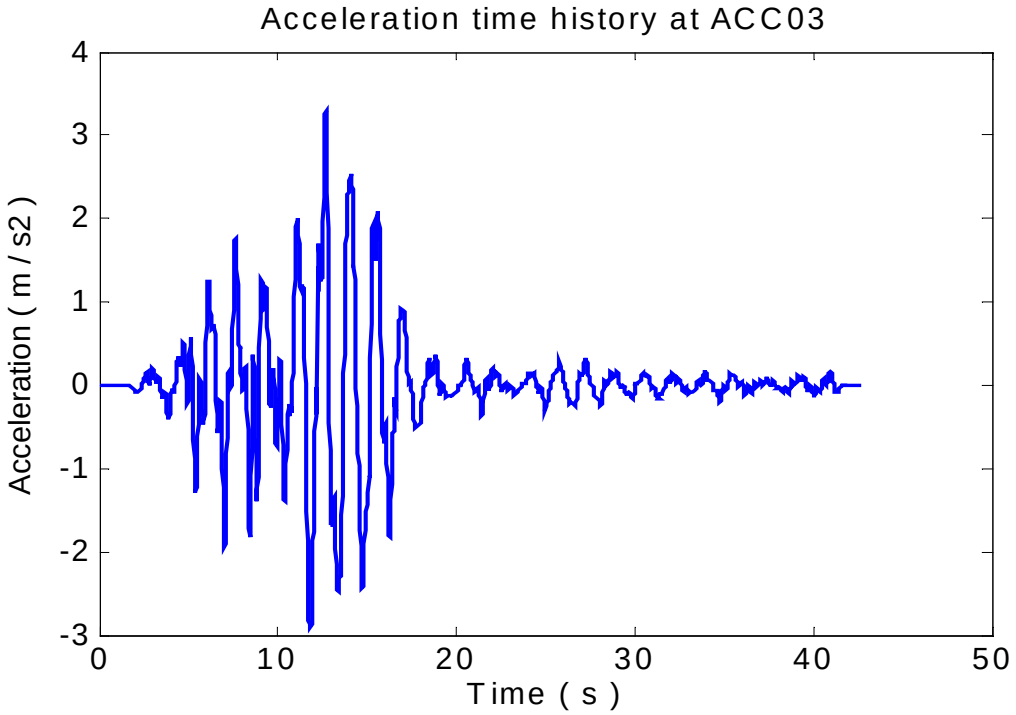

Fig. 19 Predicted ACC03 time history

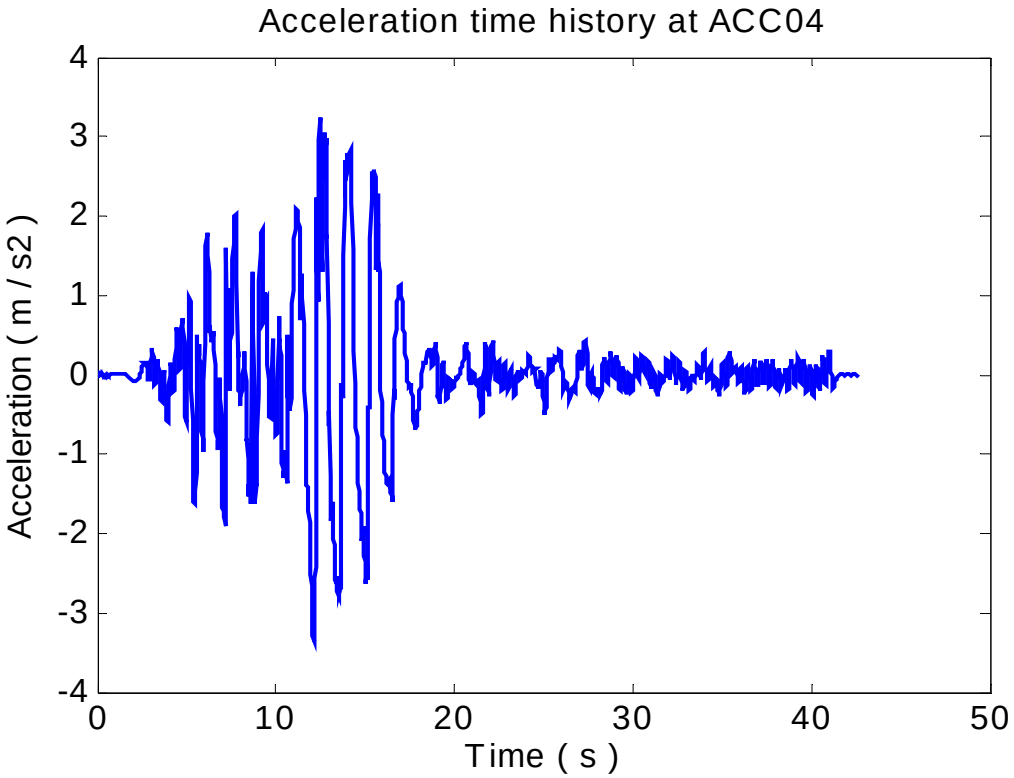

Fig. 20 Predicted ACC04 time history

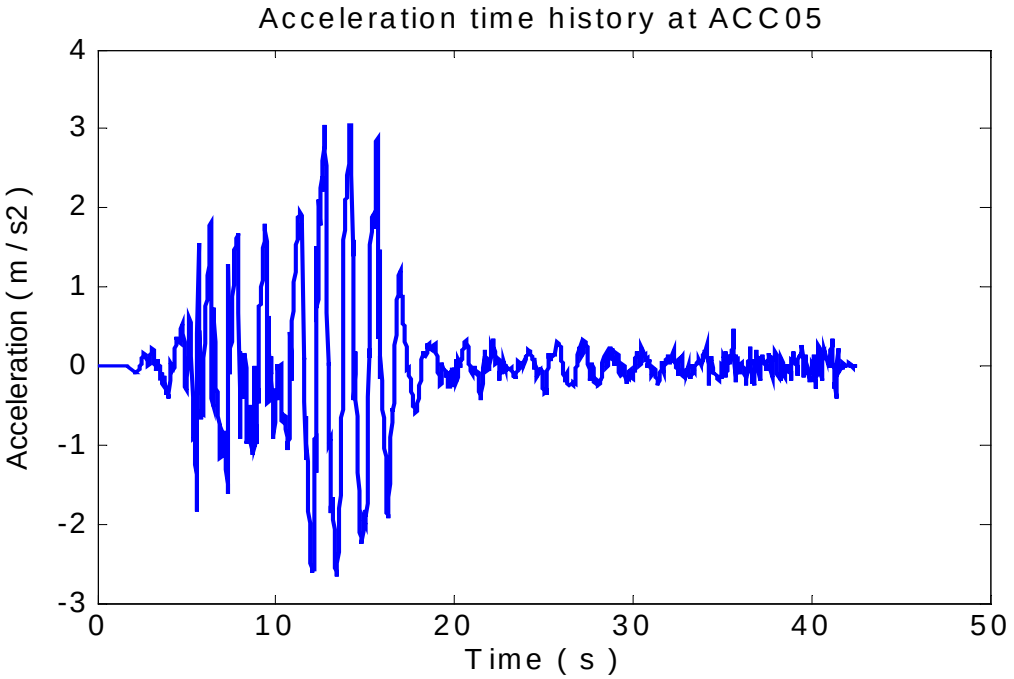

Fig. 21 Predicted ACC05 time history

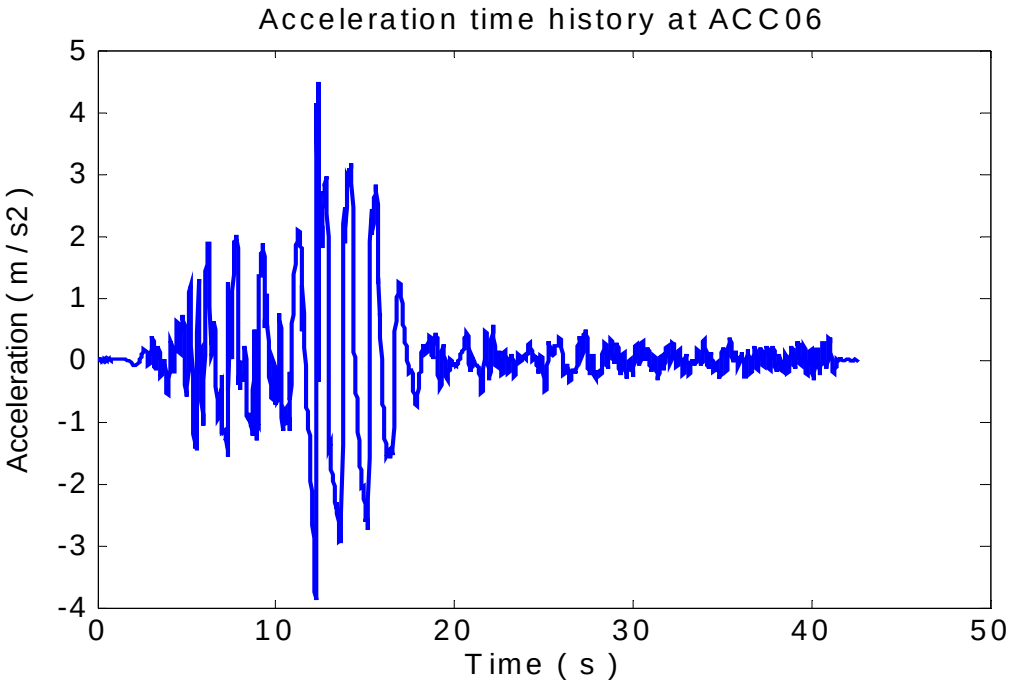

Fig. 22 Predicted ACC06 time history

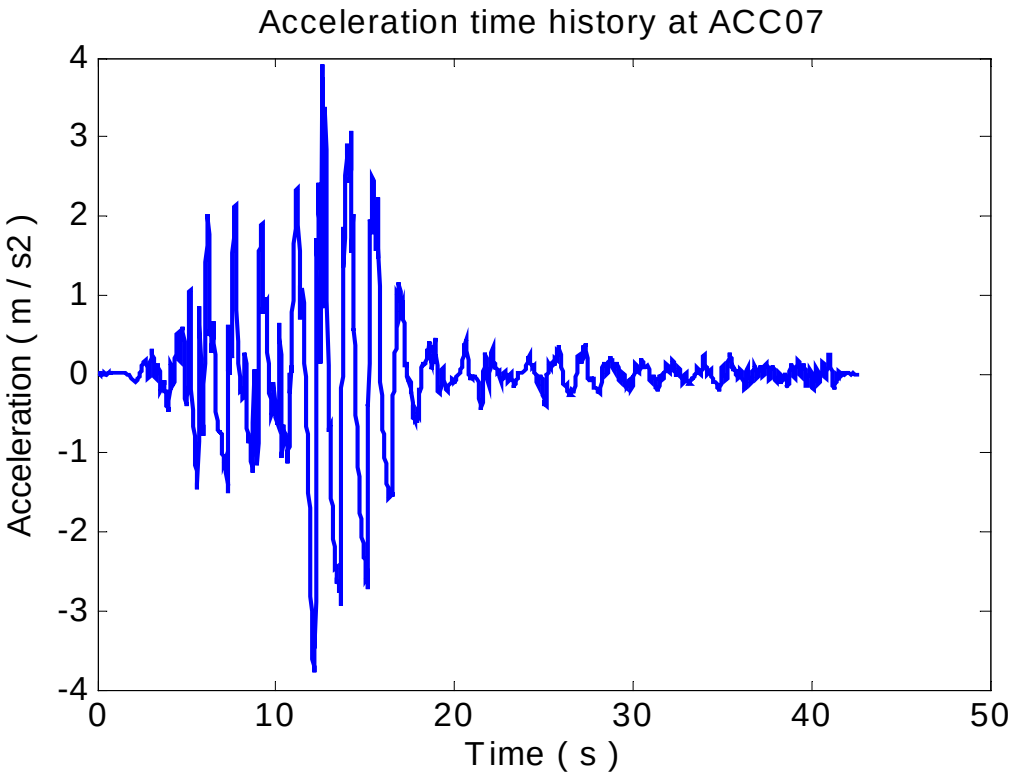

Fig. 23 Predicted ACC07 time history

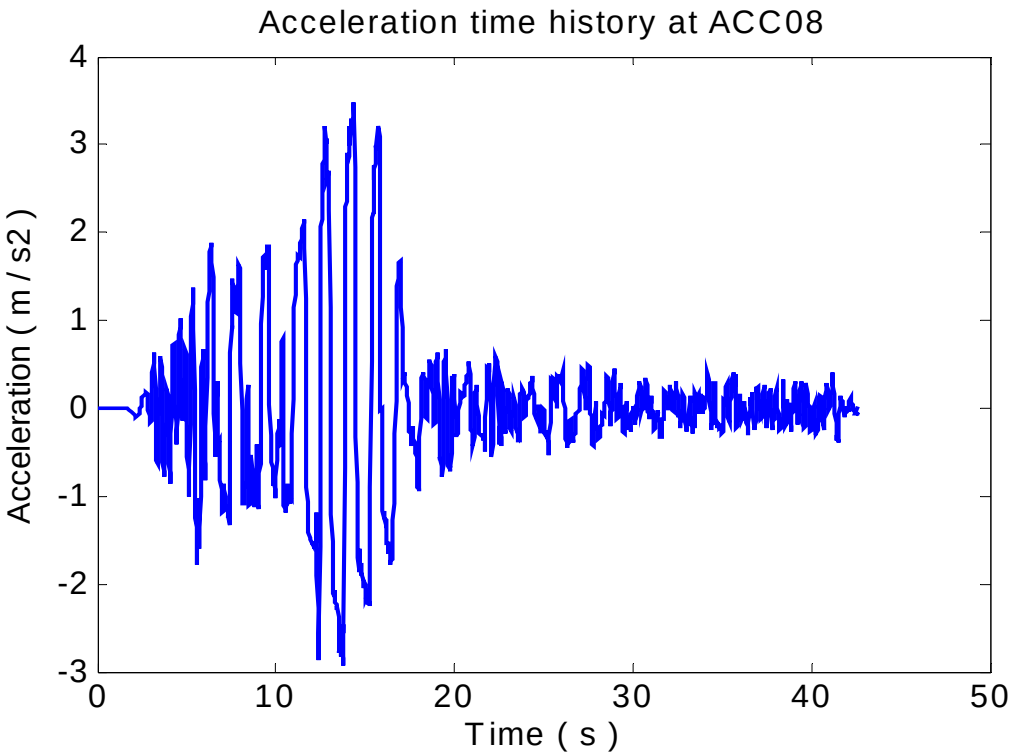

Fig. 24 Predicted ACC08 time history

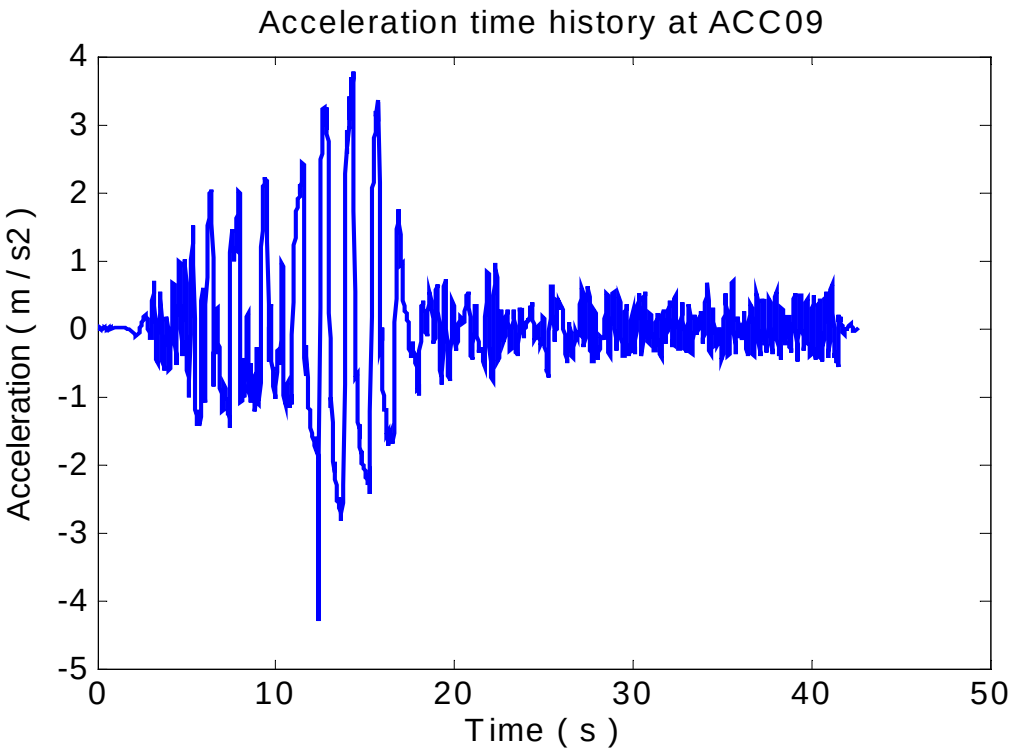

Fig. 25 Predicted ACC09 time history

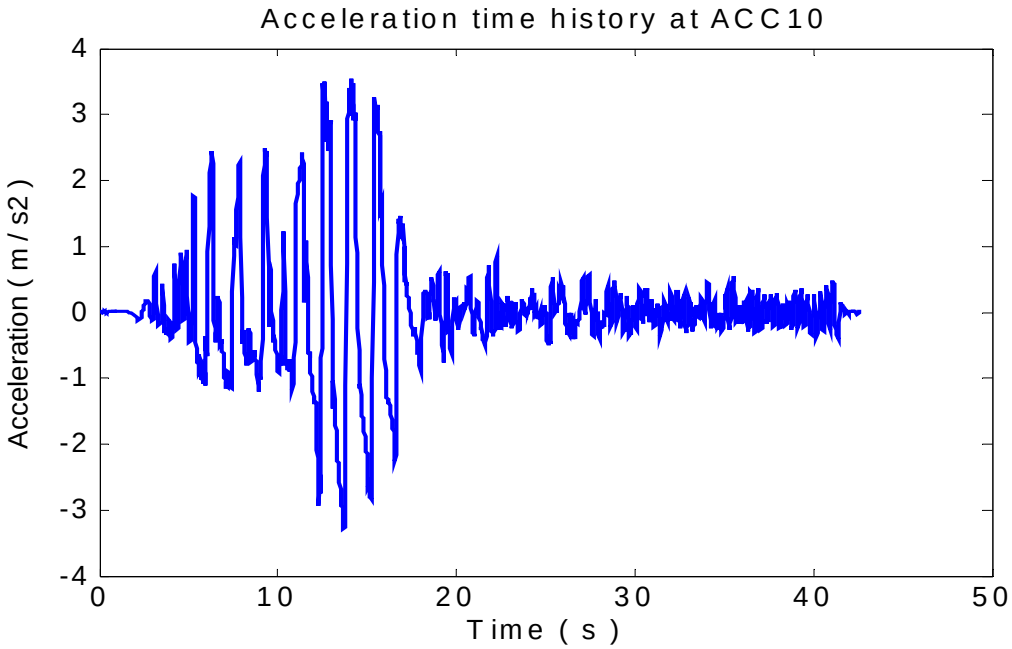

Fig. 26 Predicted ACC10 time history

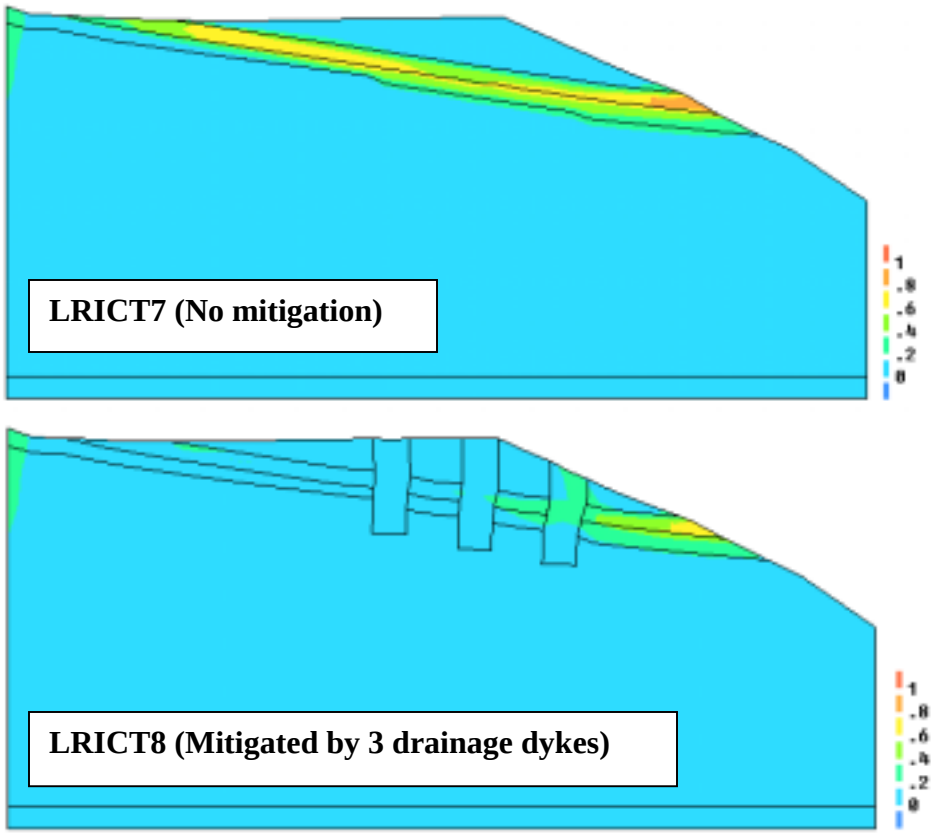

Fig. 27 Comparison of the predicted maximum shear strain contours in tests 7 and 8 at the end of analysis, t= 42.54 s. (Deformed shape magnification factor=1)

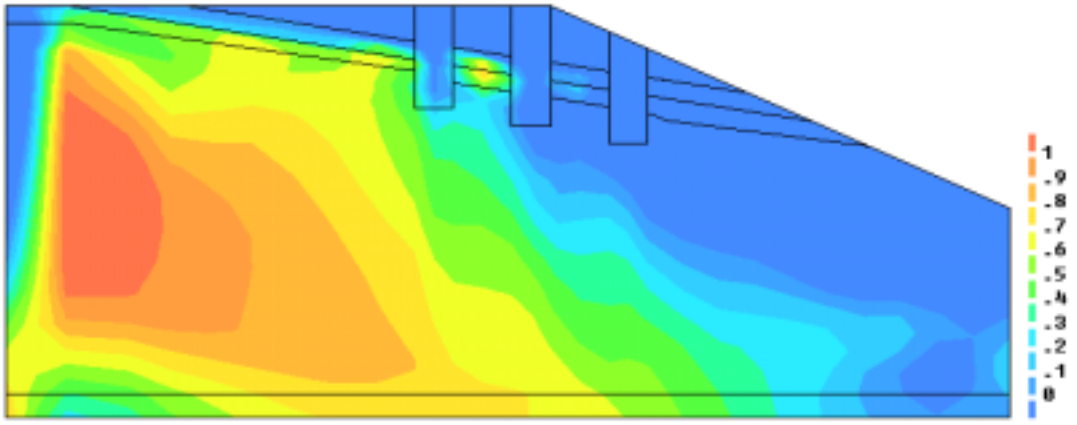

Fig. 28 Predicted excess pore water pressure ratio contours at t= 14 s

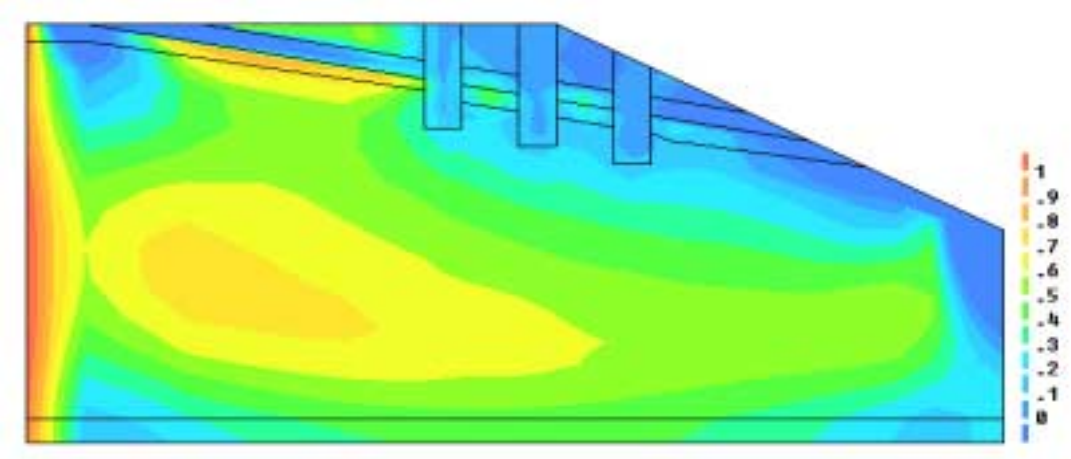

Fig. 29 Predicted excess pore water pressure ratio contours at t= 20 s

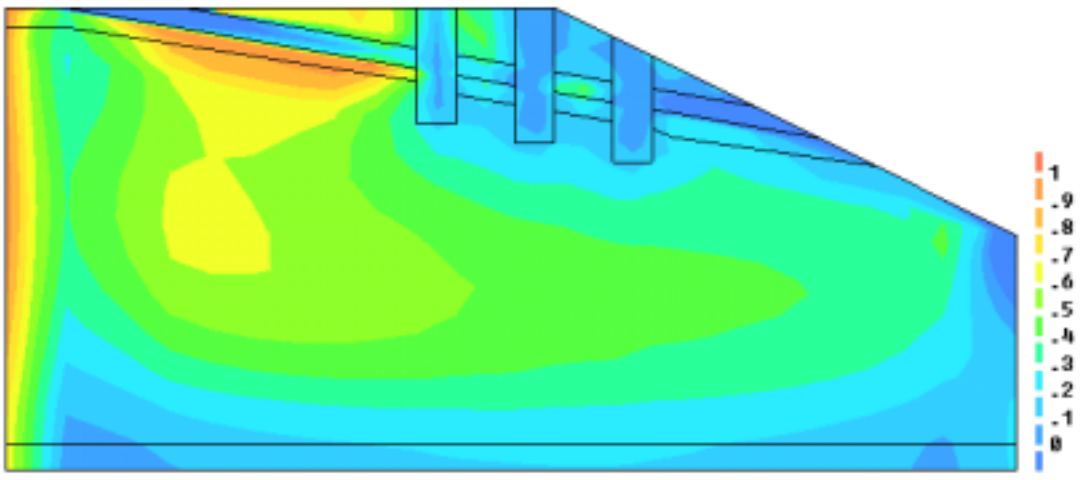

Fig. 30 Predicted excess pore water pressure ratio contours at t= 28 s

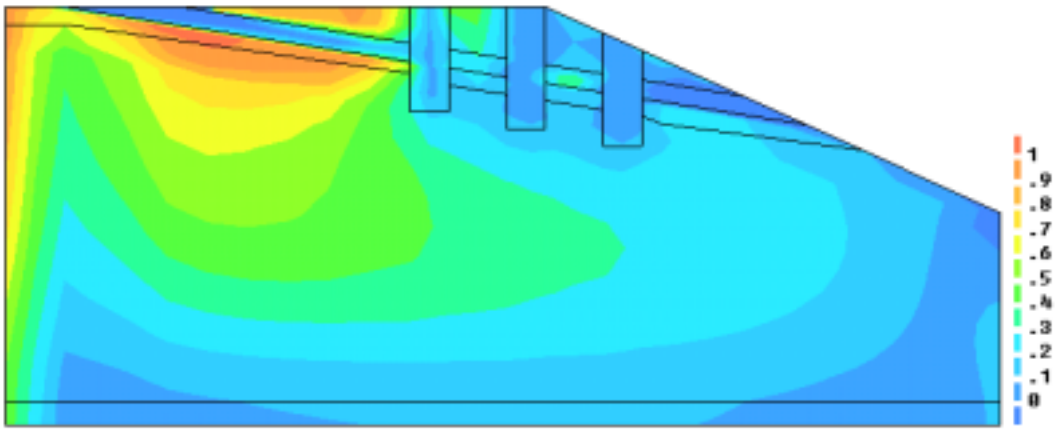

Fig. 31 Predicted excess pore water pressure ratio contours at t= 36 s

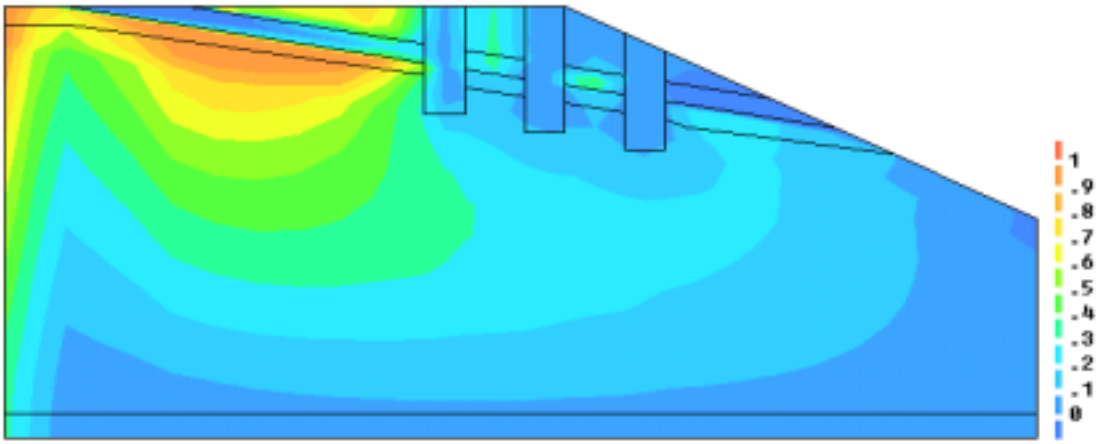

Fig. 32 Predicted excess pore water pressure ratio contours at the end of analysis (t= 42.54 s)

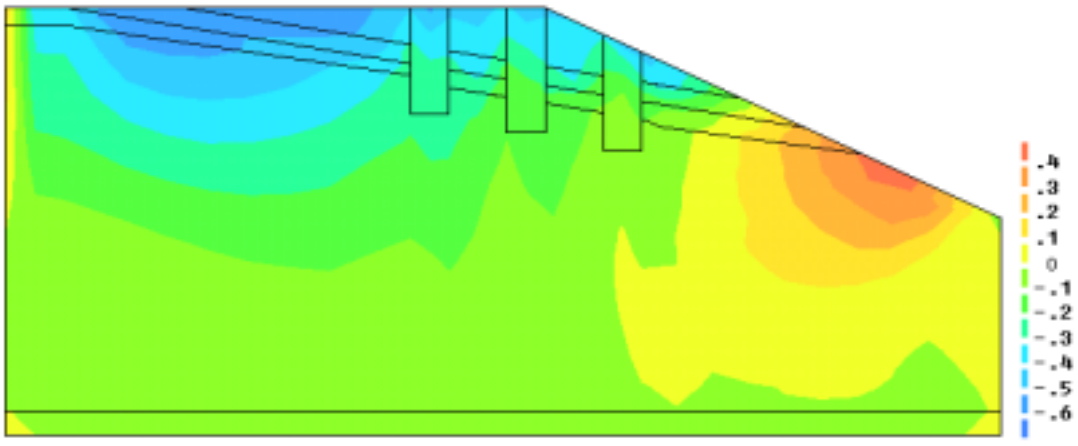

Fig. 33 Predicted vertical displacement contours at the end of analysis (t= 42.54 s)